

Heat transfer analysis of air flow through irregular geometric ducts

Dhurgham H. Talib*, Rafel H. Hameed, Adil A. Alwan

University of Babylon / College of the Engineering / Department of Mechanical Engineering

*Corresponding author Email: dhurghamhaider1212@gmail.com

ABSTRACT

In the present work, experimental investigations have been carried out to study the effect of an irregular shape geometry duct on the heat transfer and fluid flow characteristics. During the study, it was measured the temperature distribution, and air velocity through a duct with the different cases study of boundary conditions. The main part of the duct is designed with dimensions 3.65 m length, 0.4 m width, 0.5 m height, and 1mm-thickness. Three duct components: length 1.25 m, width 0.4 m and height 0.25 m for the entrance section, length 1.2 m for the test section and length 1.25 m, width 0.4 m and height 0.5 m for the exit section. Ductwork is made of galvanized steel. Galvanized was a standard, most common material used in fabricating ductwork for most comfort air conditioning systems. The specifications for the galvanized steel sheet are ASTM A653, coating G90. The inlet duct section consists of the rectangular duct manufacturing and designed at this length to achieve a zone fully developed, the test duct section consists of an irregular duct, and the exit duct section consists of a square duct used to minimize the exit effects of the test section. Insulation is applied to ductwork to minimize the rate of thermal loss through the metal of the duct. In a two-dimensional laminar flow, numerical simulation is carried out and the projected model deals with the distribution of temperature along the irregular duct test by numerically solving the finite difference method describing the energy equation. ANSYS - 19.2 Fluent. The flow characteristics of airflow through the irregular duct was analyzed.

KEYWORDS

heat transfer analysis, irregular geometric ducts, finite difference method, constant heat flux, temperature distribution

INTRODUCTION

The irregular duct was used to arrange inward flow and heat transfer applications in the field. Due to its workable significance, heat transfer and laminar flow in its irregular duct have received a lot of attention. In applications for heat transfer appointments, such as combustion chambers, gas turbine duct cooling, cooling sections for electronic devices, and interior cooling for engines and nuclear power reactors, channels with an irregular cross-section are typically used, embedded heat exchangers, and fuel cells. These devices must be compressed as long as the heat transfer to the environment is rapid. The application of this kind of duct is becoming more and more common. It is very important to be able to prophesy heat transfer and the pressure drop characteristics of fluid flows in the irregular duct. Numerous studies have been performed on laminar flow in straight and irregular channels presented in the past. Chen et al. investigated heat transfer through irregular channels with cross corrugation and the use of uniform boundary conditions for heat flow was achieved [1]. The Results of the coefficient of friction and a Nusselt number obtained from experiments and simulations exhibit that the flow in the duct has the greatest Nusselt number and friction factor.

K.Sivakumar et al. studied systematic experimental heat transfer and pressure drop comparison between smooth and three different sized square ribbed divergent rectangular ducts [2]. The results obtained from the ribbed ducts were compared with that of the same parameter smooth (without ribs) divergent rectangular duct. The enhanced heat transfer rate for the 3 mm height rib divergent rectangular duct is more than 6, 9 mm rib height rectangular divergent duct, and smooth duct. For pressure drop point of view, 6 and 9 mm rib height is higher than 3 mm and smooth duct respectively. Zhang and Chen studied the fluid flow and heat transfer in a cross-corrugated triangular

duct under uniform heat flux boundary condition was modeled and experimentally studied [3]. In order to validate the model, heat transfer tests and a high-speed measurement system for hot wire strength are used. Onur and Arslan investigated experimentally of steady-state laminar forced flow and heat transfer in a horizontal smooth trapezoidal duct having different corner angles in the Reynolds number range from 102 to 103 [4]. Flow is hydrodynamically fully developed and thermally developing under a uniform surface temperature condition. Results have shown that the heat transfer rate increases as the Reynolds number increases, but the friction factor of Darcy decreases.

It is also observed that with the rising corner angle of the duct, the average Nusselt number increases while the average Darcy friction factor decreases. Renksizbulut and Niazmand investigated simultaneously developing three-dimensional laminar flow and heat transfer in the entrance region of trapezoidal channels using numerical methods in the Reynolds number range from 10 to 1000 [5]. The principal and secondary velocity fields, the temperature field, and all associated heat and momentum exchange parameters have been examined. It is shown that boundary-layer type of approximations, which lead to Reynolds number-independent Poiseuille and Nusselt numbers, can be used for Reynolds numbers over 50 and after a few hydraulic diameters from the channel inlet. It is also shown that hydrodynamic entrance lengths calculated with methods based on fully developed flow data are grossly in error. Bhadouriya et al studied experimentally Characteristics of heat transfer and friction factor for airflow inside a square duct and through 3D numerical simulation under uniform Condition of wall temperature limits, twist ratio of 11.5 and 16 .5, and Reynolds number 600–70,000 [6].

The local distribution of the ratio of the friction factor and the Nusselt number across the cross-section has been shown. Based on the parameters of constant pumping power, the reinforcement factor is determined to compare the twisted channels with the straight ones. Selections of twisted square ducts are presented in terms of enhancement factors. It was found that the convoluted ductworks well in laminar. Liu and Wang investigated The current work on bifurcation and stability is fully developed in a tightly curved rectangular duct [7]. The stability of the flow on the different branches is determined through a straightforward transient calculation on the dynamic responses of multiple solutions. As the number of deans increases, finite random disturbances lead to flows, cyclic oscillation, periodic oscillation, other cyclic oscillation, and chaotic oscillation from one steady state to another steady state. For all physically possible fluxes, the average friction factor and the average NSLT number are obtained. Zhang and Wan studied numerically Laminar flow and thermal transfer in rectangular cross-section trapezoidal channels [8]. In some conditions, the distribution of the temperature difference and the pressure drop in the trapezoidal channels is stronger than those in the rectangular channels, contributing to the benefit of improving the transfer of heat.

Using the Taguchi form, the applicability of the assumptions above was demonstrated. Tokgoz and. Sahin determined the flux characteristics and thermal efficiency of different duct engineering numerically and experimentally [9]. Experimental experiments were performed using the particle image velocity (PIV) technique to describe the hydrodynamic structures and validate the numerical solution outcomes. Experimentally and numerically, speed distributions, rheological patterns, and corresponding turbulent statistics were calculated to reveal the hydrodynamic properties and thermal efficiency of the corrugated channel flow. Norouzi et al. studied Creeping flow and inertial fluid in a curved duct with a square cross-section [10]. To examine fluid flow, numerical modeling was used, and the governing equations were calculated using the method of finite difference on an overlapping network. The effect of the centrifugal force on the flow field was studied due to channel curvature and the opposite effects of the first and second normal pressure difference. Furthermore, to extract the force balance relationships for the primary flow field, the volume ordering technique is used. On the basis of these relationships, the centrifugal force output mechanism and the normal variation in the pressure producing secondary flows are regarded as.

Mohammad Mohsen et al. obtained for the first time an accurate analytical solution for heat transfer in straight ducts with rectangular cross-sections [11]. This solution is true for boundary conditions relating to fully defined heat transfer in the duct walls under continuous heat flow. To find the closed form of the temperature distribution, the method of separating variables and various other mathematical techniques are used. As the aspect ratio functions, local and average NSLT numbers are also obtained as. Khatri and Agarwal analyzed Numerical

simulation of laminar flow in a parallel plate channel for different entry velocity using the finite element method by solving partial differential equations of fluid flow [12]. Fluid flow is expressed by a partial differential equation (Poisson's equation). The effect of the presence of heat flux outside the field on the temperature flux field was also examined. Analyses are conducted for various entry velocity values by observing the flow field and the temperature and pressure field. The results showed that the change in entry velocity significantly affected fluid flow, temperature flow, and pressure. Chiu et al studied of Heat transfer in horizontal channels having radioactive forcing was examined in detail [13].

This study mainly focuses on the interaction of thermal radiation in rectangular horizontal channels with the mixed convection of a gray liquid. To solve the three-dimensional Navier - Stokes equations and the energy equation simultaneously, the vortices-velocity approach is used. A discrete coordination process solved the equation for integrated differential radioactive conversion. The results concentrate on the effects of thermal buoyancy on the evolution of temperature, friction factor, and Nusselt number. Farhanieh and Sunden examined numerically the simultaneously developing laminar flow and heat transfer in the entrance region of a straight trapezoidal duct under constant wall temperature boundary condition using the finite-volume method [14]. Using common-site variables and Cartesian velocity elements, the governing equations are solved numerically by formulating a finite volume in complex three-dimensional geometries. Details of the numerical method are shown. Ghobadi and Muzychka reviewed the heat transfer and pressure drop correlation of a fully developed laminated Newtonian fluid flow in the curved channel [15]. Curved engineering is one of the methods of promoting passive heat transfer that is suitable for many heat transfer applications such as power production, chemical, and food industries, electronics, environmental engineering, etc.

The main purpose of this review paper is to provide researchers with a comprehensive list of correlations and concepts that they may need during their research. Zhang interested in the development of a low Reynolds number heat exchanger system, laminar flow inside a rectangular duct [16]. Heat transfer from a rectangular cross-section with different aspect ratios to thermally formed and dynamically developed inside an air duct has been well researched and reported in different books, but not much work has been done for the lamellar fin ducts. The Nusselt figures in the developed area are obtained, The heat input length, and fully defined values for these paths, which can be used to estimate the efficiency of heat transfer of finned heat exchangers with different thermal conductivities and thickness. Sadasivam et al modeled laminar, which is entirely developed using single and hexagonal channels [17]. To map the irregular cross-section on a rectangular arithmetic field, a coordination transformation is used. Thermal boundary conditions are called since, in most practical applications, they reflect the basic deciding conditions. For a broad range of airway aspect ratios and with four distinct trapezoidal angles, solutions to changes in velocity and temperature are obtained. The results of the friction coefficient and the Nusselt number indicate heavy dependency on the geometry of the duct. Ray and Misra employed the least-squares point matching technique to investigate laminar, fully developed through triangular and square channels with round corners for two types of boundary conditions, namely, constant axial heat input and uniform peripheral wall temperature, and uniform axial, as well as, peripheral heat input [18]. They concluded that with increasing the radius of the round corners, the friction factor and the electivity of the round portion for each of the considered duct geometries increased quickly.

EXPERIMENT SETUP

A schematic diagram of the experimental setup for heat transfer analysis is shown in Figure (1). The duct has an internal size of 4.5 m x 0.4m x 0.2m which consists of an entrance section, test section, and exit section was used to perform heat transfer and pressure drop experiments. It is an open inlet duct system comprising of five main components: a variable speed blower, a wind tunnel, an upstream section, a test section, and a downstream section. The air-conditioned indoor air is supplied to the tunnel by a centrifugal variable speed blower that pulls air into a geometrical duct. It has an electrical motor with specifications 800 watt, 220 volts, and frequency 50 Hz. It has a range velocity between (2 m/s to 7m/s) as shown in figure (2). The volumetric airflow rates can be adjusted to have different Reynolds number. The low-speed wind tunnel is to ensure a continuous, steady air supply. A hand-held digital anemometer is used to measure the speed of airflow through the duct as shown in figure (3). In the test section, a heat exchanger in the form of an irregular duct is flanged between the upstream and the downstream sections Thermal couples, type K and 1.5 mm in diameter, was attached to the inner surface to measure

the temperature. The temperatures that were measured are then averaged transversely across the y-axis to have the transversely local mean temperatures along the duct. Uniform heating is produced on the outer surfaces of the copper plates by means of an electrically heated chrome heater wire (0.5 mm thick) that is wrapped uniformly around the outer surface of the test portion of the duct. The electrical heater was considered the source of heat flux on the surfaces of the test section. It was made from Nickel Chrome alloys consist of six turns and connected with a power analyzer device to supply currents. To control the value of the power supply to the heater, a variable voltage device was used. This device can supply different values of voltage with a range of (0 to 220) volts. This variation is regulated by changing the internal resistance until, as shown in the figure, it reaches the appropriate voltage value figure (4). The Lutron style digital power analyzer (DW-6091) with a maximum current (10 A) and maximum voltage (600 V) is used to convert the (analog) voltage signal from the power supply into a digital signal that can be read as shown in the figure (5). To minimize heat loss, the duct was insulated. The experimental rig photograph is shown in Figure (7)

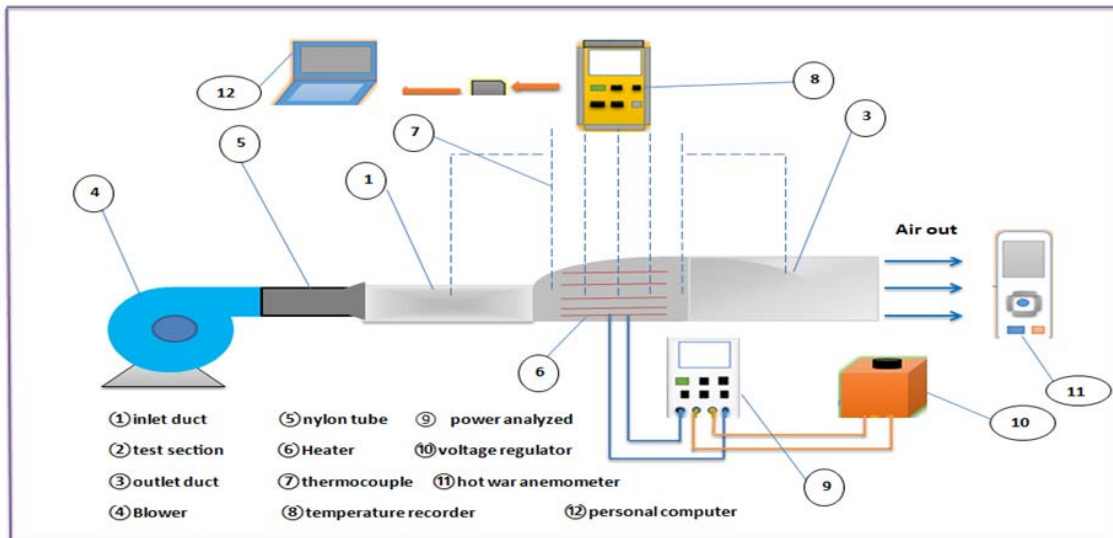


Figure 1. schematic diagram of the rig test

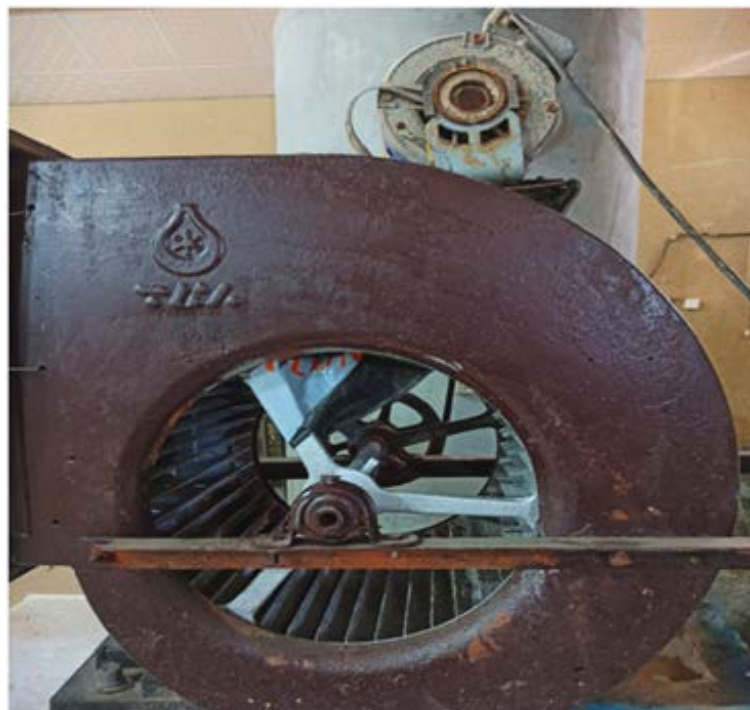


Figure 2. Centerfugal blower



Figure 3. Hand-held digital anemometer



Figure 4. Photograph of Voltage Variation Device

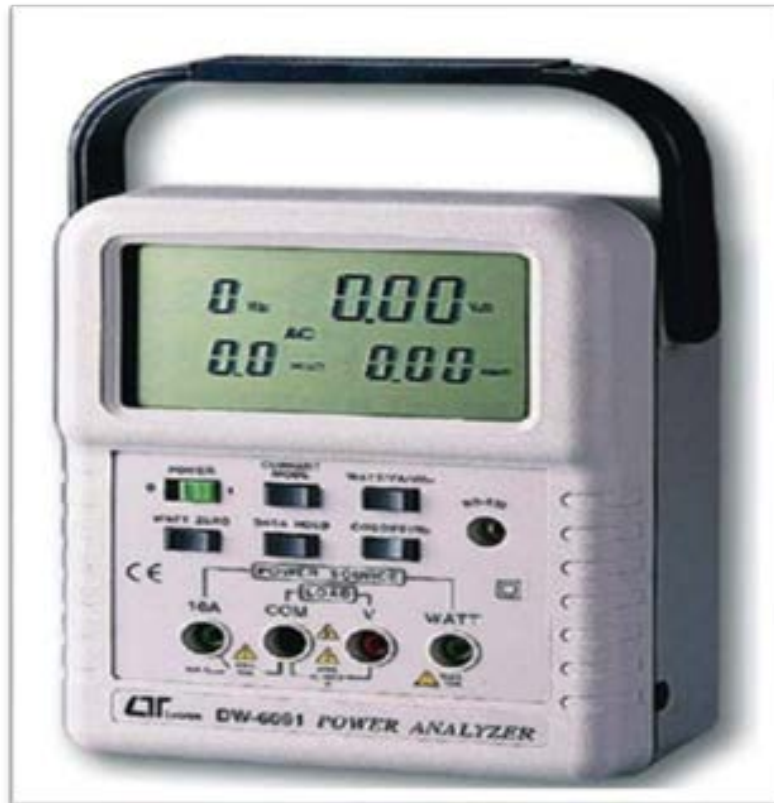


Figure 5. Photograph of power analyzer device



Figure 6. Photo of temperature measuring device

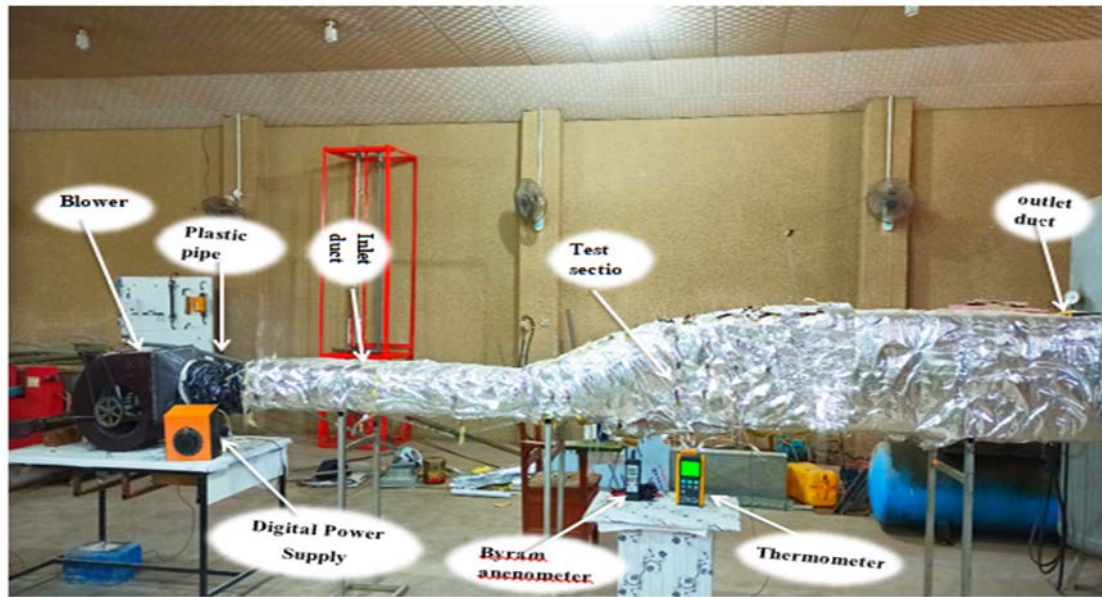


Figure 7. Photograph of experimental rig

GOVERNING EQUATIONS

With the assistance of incompressible, time-independent continuity, momentum, and energy equations, the flow of air through the duct is calculated as shown in eq. Based on the law of physical conservation, these equations are formed. The continuity equation is derived from mass conservation, the momentum equation is the steady-state incompressible flow Navier-Stokes equation, and the energy equation is used to determine the heat transfer due to the change in air temperature.

Continuity equation

$$\partial u / \partial x + \partial v / \partial y = 0 \quad (1)$$

Momentum Conservation

For fully developed laminar flow in ducts, the momentum is governed by:

$$\mu \left(\frac{\partial^2 u}{\partial x^2} + \frac{\partial^2 u}{\partial y^2} \right) = \frac{\partial P}{\partial z} \quad (2)$$

Where μ is dynamic viscosity (Pa s), u is fluid velocity (m/s), P is the pressure (Pa), z is the axial coordinate (m), and P is pressure (Pa).

Energy Conservation

$$\rho C_p u \frac{\partial T}{\partial z} = \lambda \left(\frac{\partial^2 u}{\partial x^2} + \frac{\partial^2 u}{\partial y^2} \right) \quad (3)$$

where T is fluid temperature (K), k is thermal conductivity (kW/m K), ρ is density (kg/m³), and c_p is specific heat (kJ/kg K)

DESCRIPTION OF AIR FLOW THROUGH DUCT

The airflow definition can be seen in Figure (8). The left side is the inlet duct from which air reaches the inner duct while the completely formed speaks in the inlet duct, the right side is the outlet duct through which air exits it and there is an abnormal duct between the inlet and outlet duct test segment.

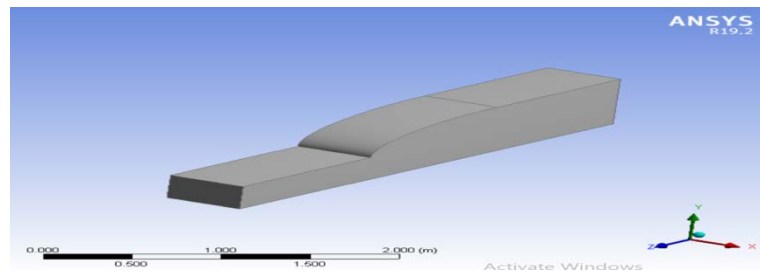


Figure 8. Duct geometry by ansys

The Geometry

Using Design modeler combined with Ansys Workbench 19.2, the geometry of the device was modeled as a 2D structure for the two-phase flow by drawing inlet duct rectangular on the X-Y plane with (40cm) horizontal and irregular duct with quarter ellipse on top and length (120cm), and exit duct with dimension (40X50X120), a surface was built from the sketch. Fluid was set to be the geometry. It was appropriate to construct it as small as possible for the purpose of obtaining an inexpensive arithmetical model, but it should be large enough to overcome all the flow and energy that affects heat transfer.

The Mesh

There are several forms of mesh, such as coarse, medium, and fine mesh. In this work, the geometry of the duct was divided into a small square element (Quadrilateral structured grid) using the meshing combined with Ansys Workbench 19.2 with a maximum and minimum size equal to (0.002 m) by fine elements (Quadrilateral structured grid) using the meshing combined with Ansys Workbench 19.2. and straight to give Y^+ less than 5 to solve the laminar sub-layer. The model governing equations would be solved at each element of the model geometry. As shown in figure (9).

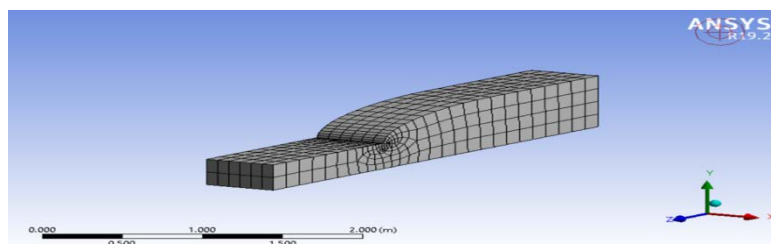


Figure 9. Mesh of duct

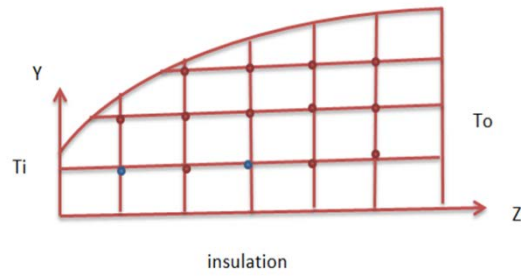
ASSUMPTION

Some simplifying assumptions are also required before applying the conventional flow equations and energy equations to model the flow and heat transfer process in the irregular duct. The major assumptions are:

- (1) When the airflow through the duct, the properties of the air can be seen as constant.
- (2) The flows inside the ducts are considered to be incompressible and steady.
- (3) Thermal radiation and nature convection are neglected.
- (4) Two dimensions in X and Y direction
- (5) No heat generation $q'''=0$
- (6) Steady-state $\partial v/\partial y = 0$
- (7) Isentropic properties (constant thermal conductivity) K is constant

BOUNDARY CONDITION

$$q'' = -k \frac{\partial T}{\partial y}$$



- 1- $T(0,y)=T_i$
- 2- $\partial T/\partial y(z,0)=0$
- 3- $k \partial T/\partial y(z,40)=q''$
- 4- $T(120,y)=T_o$

MATHEMATICAL MODEL

Heat transfer through fenestration systems can be modeled mathematically by the formulation of the governing equations derived from the Conservation of Mass, Newton's Second Law, and the First Law of Thermodynamics. The governing equations are written in terms of local velocity components, pressure, and temperature. Equations that govern convection, conduction, and radiation heat transfer, together with the appropriate boundary conditions, constitute a complete mathematical model of heat transfer through fenestration systems. Using finite difference approximation to solve the partial differential equation (PDEs) The indices i and j were used to indicate the points along the Y and Z directions for steady-state. In the grids represented in figure (), the distance between a point in Y -coordinate is Δy and in Z -coordinate is Δz . Figure (10) represents a computational grid of the irregular model.

The partial derivative with respect to time is approximated by the forward finite difference method as: $(\partial^2 u)/\Delta y^2 + (\partial^2 u)/\Delta z^2$.

For Y -direction

$$U_{(j+1,k)} = U_{(j,k)} + \Delta y / \lambda \partial u / \partial x + (\Delta y^2) / \Delta y^2 \lambda (\partial^2 u) / (\partial y^2) \quad (4)$$

$$U_{(j-1,k)} = U_{(j,k)} - \mu \Delta y \partial u / \partial y + \mu^2 U_{(j+1,k)} - \mu^2 U_{(j,k)} - \mu^2 \Delta y \partial u / \partial y \quad (5)$$

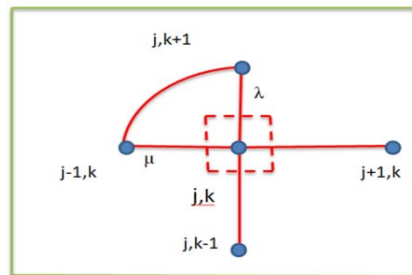


Figure 10. Nodding sketch at irregular point

From equation (4)

$$(\Delta y^2) / \Delta y^2 \lambda (\partial^2 u) / (\partial y^2) = U_{(j+1,k)} - U_{(j,k)} - \Delta y / \lambda \partial u / \partial y \quad (6)$$

Subdued equation (6) in equation (5)

$$\partial u / \partial y = (\mu^2 U_{(j+1,k)} + (1 - \mu^2) U_{(j,k)} - U_{(j-1,k)}) / (\Delta y \mu (1 + \mu)) \quad (7)$$

From equation (5)

$$\Delta y / \lambda \partial u / \partial y = U_{(j+1,k)} - U_{(j,k)} + (\Delta y^2) / 2 \lambda (\partial^2 u) / (\partial y^2)$$

Subdued in equation 4 in equation 5

$$(\partial^2 u)/(\partial y^2) = (\mu U_{j+1,k} - (1+\mu) U_{j,k} + U_{j-1,k}) / ((\Delta y^2)/2 \mu(1+\mu)) \quad (8)$$

For Z-direction

$$U_{k+1,j} = U_{k,j} + \lambda \Delta z / i \partial u / \partial z + \lambda^2 (\Delta z^2) / \Delta z^2 i (\partial^2 u) / (\partial z^2) \quad (9)$$

$$U_{k-1,j} = U_{k,j} - \Delta z / i \partial u / \partial z + (\Delta z^2) / \Delta z^2 i (\partial^2 u) / (\partial z^2) \quad (10)$$

From equation (10)

$$(\Delta z^2) / \Delta z^2 i (\partial^2 u) / (\partial z^2) = U_{k-1,j} - U_{k,j} + \Delta z / i \partial u / \partial z \quad (11)$$

Sub equation (11) in equation (9)

$$\partial u / \partial z = (U_{k+1,j} + U_{k,j} (\lambda^2 - 1) - \lambda^2 U_{k-1,j}) / (\lambda (\lambda + 1) \Delta z) \quad (12)$$

From equation (10) Sup in equation (9)

$$(\partial^2 u) / (\partial z^2) = (U_{k+1,j} - U_{k,j} (\lambda + 1) + [\lambda U]_{k-1,j}) / (\lambda (\lambda + 1) (\Delta z^2) / \Delta z^2 i) \quad (13)$$

For centriel nodes

$$(\partial^2 u) / dy^2 + (\partial^2 u) / dz^2 = 0 \quad (14)$$

$$(U_{j+1,k} - 2U_{j,k} + U_{j-1,k}) / dy^2 + (U_{k+1,j} - 2U_{j,k} + U_{k-1,j}) / dz^2 = 0 \quad (15)$$

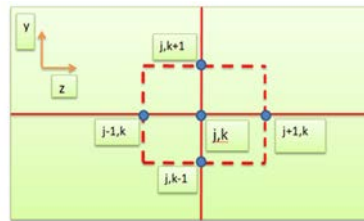


Figure 11. Nodding sketch at central point

Reynolds number can be found as:

$$Re = (\rho U D_h) / \mu$$

Where:

D_h was the hydraulic diameter of the channel

μ was the viscosity of the fluid

ν was the kinematic viscosity of the fluid

U was the mean fluid velocity of air

ρ was the density of air

The hydraulic diameter was calculated where A_x was the cross-sectional area, p was the perimeter, H was the channel height, and W was the channel width:

$$D_h = (4A_x) / P = (2HW) / (H+W)$$

Nusselt number (Nu) is generally expressed as

$$Nu = (h D_h) / k$$

Mathematically, the Darcy Weisbach equation may be used to determine the pressure drop in ducts.

$$\Delta P = f^* \rho^* l / D^* v^2 / 2g$$

The primary indicator used to compare frictional losses was the Fanning friction factor, f . The formula used to calculate the Fanning Friction Factor is given in Equation 5.10 where ΔP was the pressure drop between the two pressure taps and L was the distance between the taps.

$$f = \Delta P / (2(L/D_h) \rho U^2)$$

RESULTS AND DISCUSSION

This study aims to determine heat and fluid flow Static properties, laminar, and both Fully optimized flow dynamically and thermally through an irregular duct. Calculations are made for air as a working fluid With Prandtl number 0.7. To study, the effect of velocity on heat and fluids For flow, its three different values are considered: 5.8, 3.5 and 2 m/s the primary indicator used to compare friction losses was the Fanning Friction Factor, f . The equation used to calculate the fan friction factor is given in Equation 5.10 where P was the pressure drop between pressure taps and L was the distance between the taps

$$.F = \Delta P / (2 (L / D_h) \rho U ^ 2)$$

This study was conducted under laminar flow conditions. After determining the temperature at different locations of the liquid in the inlet and outlet, temperatures are obtained for the bulk of the inlet and outlet. Find out the wall temperature besides the inlet, outlet, and power input temperatures of the liquid, the Nusselt average the numbers were calculated. Also, the mean Darcy friction coefficient was estimated to determine the pressure drop in the test channel. The experimental results were presented in non-dimensions Nusselt number and Darcy friction factor for each angle. Average Nusselt number, mean Darcy friction factor, and Reynolds numbers for flow in this channel

It adopts hydraulic diameter D_h .

Figure (12) shows the relationship of the air velocity passing inside the duct and the X-axis, that it was an increase in the air velocity in the middle of the duct at the beginning of the entry, and the speed gradually decreases when passing in the second irregular zone

Figure (13), figure (14), and figure (15) shows the relationship between the temperature of the air inside of the test irregular duct and along the x-axis at a deferent velocity of air For three different y-axis locations, that it was the temperature increases when it is near the heater

Figure (16), figure (17), and figure (18) shows the relationship between Nusselt number and Reynolds number was drawn to investigate the effect of the velocity on coercive force convection heat transfer.

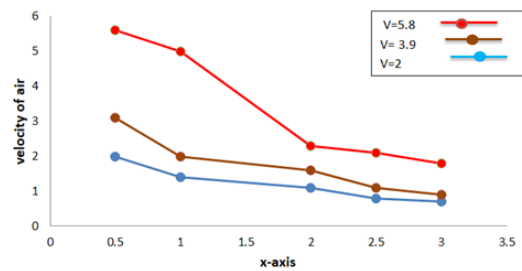


Figure 12. Velocity with X-axis

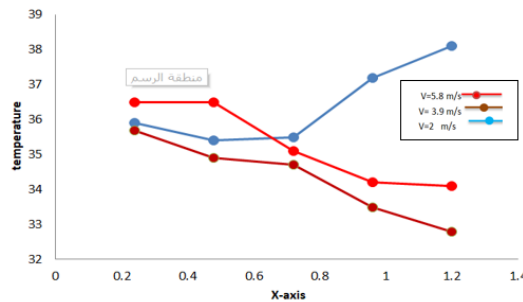


Figure 13. Temperature with X-axis at $y_1=6.5\text{cm}$ and $y_2=13.5\text{ cm}$

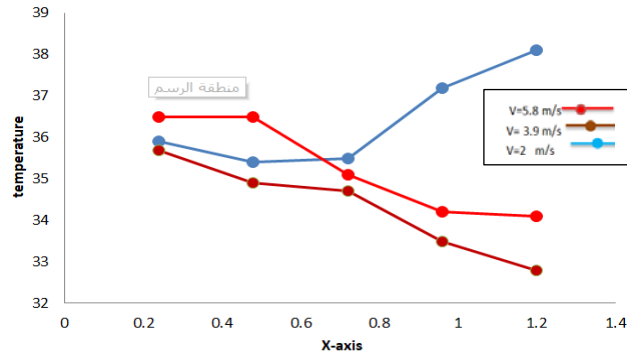


Figure 14. Temperature with X-axis at y1=13cm and y2=27 cm

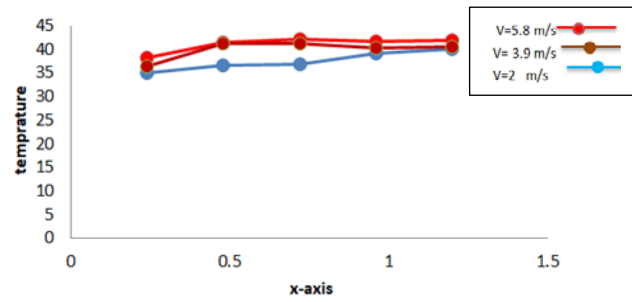


Figure 15. Temperature with X-axis at y1=19.5cm and y2=40.5 cm

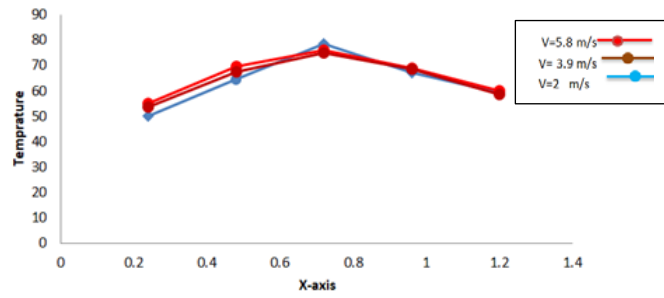


Figure 16. Variation of average Nusselt number with Reynolds number at velocity 5.8 m/s

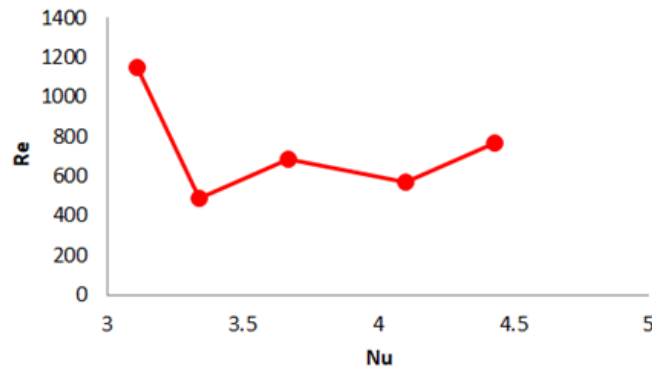


Figure 17. Variation of average friction factor with Reynolds number at velocity 5.8 m/s

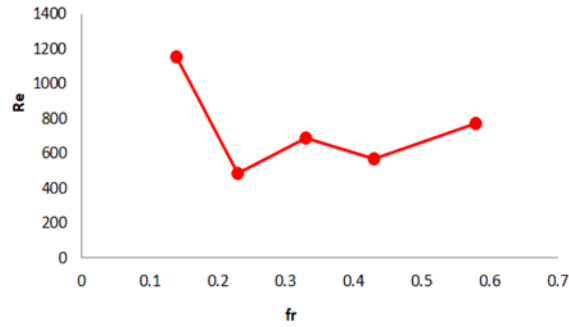


Figure 18. Variation of average Nusselt number with Reynolds number at velocity 3.9 m/s

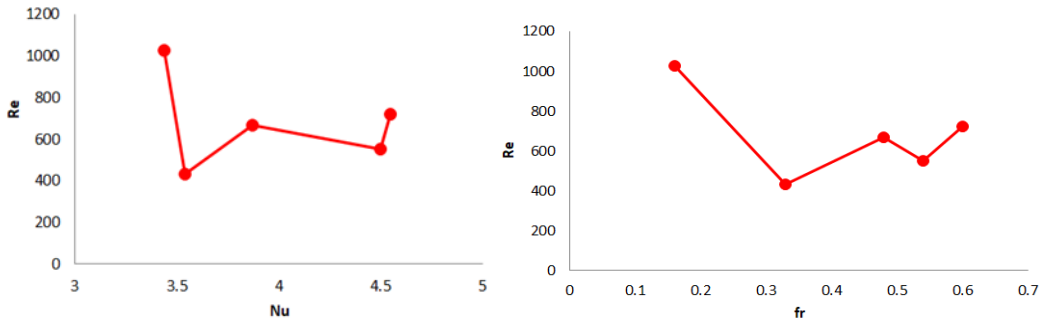


Figure 19. Variation of friction factor with Reynolds number at velocity 3.9 m/s

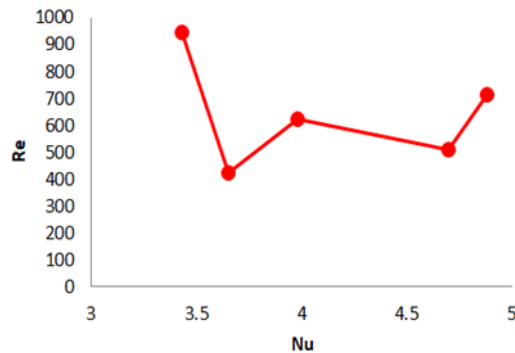


Figure 20. Variation of average Nusselt number with Reynolds number at velocity 2 m/s

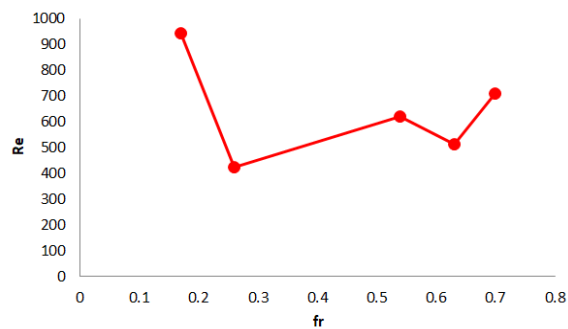


Figure 21. Variation of average friction factor with Reynolds number at velocity 2 m/s

Figure (19), figure (20), and figure (21) it shows the relationship between average friction factor and Reynolds number was drawn to investigate the effect of the velocity on coercive force convection heat transfer. With the rising Reynolds number for all types of winglets used at all relative longitudinal pitches, the friction factor decreases. For a relative longitudinal pitch of 6, the friction factor was found to be the lowest, followed by 5, 4 and a maximum of 3, respectively. Each number displays the experimental values of the average friction factor.

The number and average of Darcy's friction factor for different velocity over the range Reynolds number from 450 to 1400. The velocity's varied, such as 5.8,3.5 and 2 m/s.

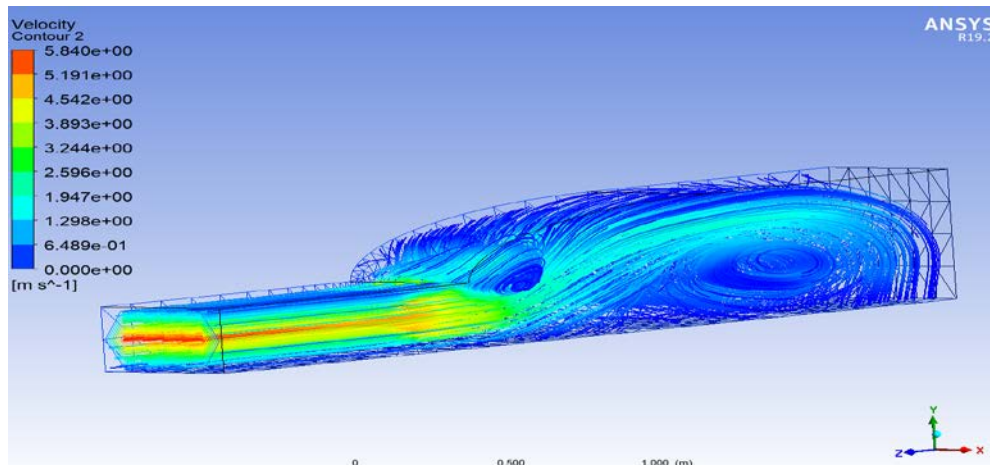


Figure 22. counter of velocity through duct

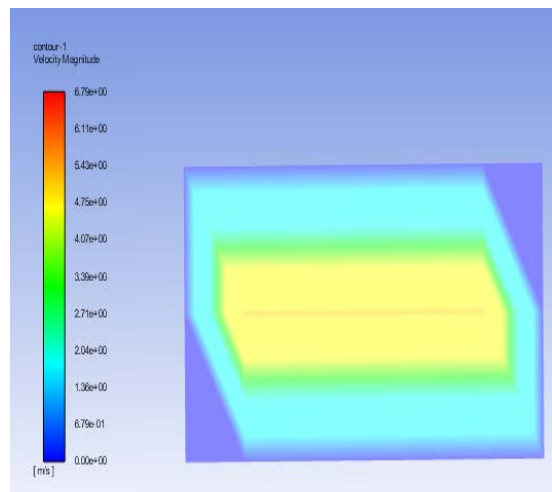


Figure 23. counter of velocity through inlet section outlet duct

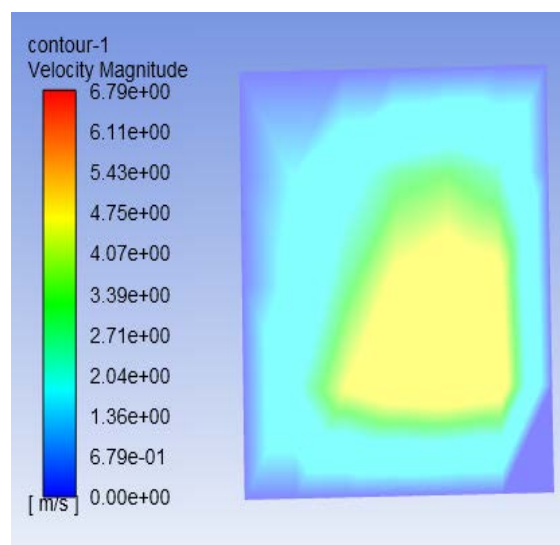


Figure 24. counter of velocity through outlet duct

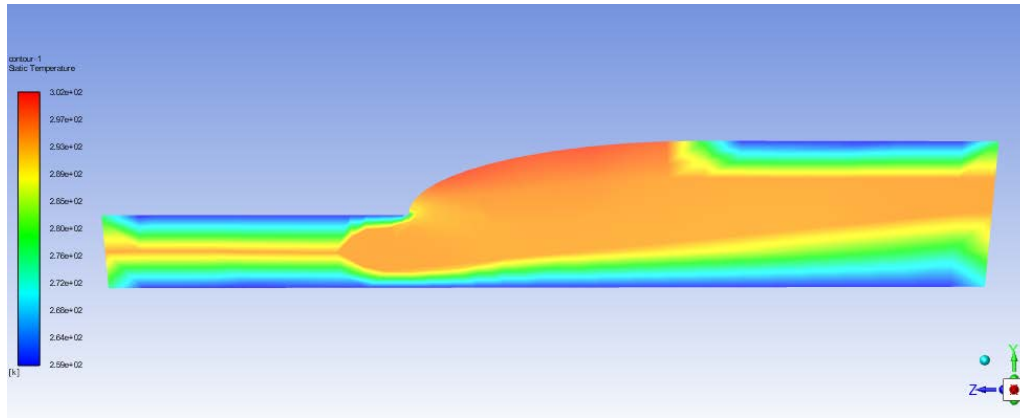


Figure 25. counter of temperature distribution through duct

CONCLUSIONS

A computational study was conducted to verify the heat transfer performance of irregular ducts. The effects of the velocity on fluid flow and heat transfer by the load in The intersecting irregular duct were examined under uniform heat flow limit conditions. Results of the coefficient of friction and a number obtained from experiments and simulations Show that flux in a duct. However, the included velocity affects the flow and heat transfer in the channels in different ways. For an irregular duct, the connection between the temperature difference and x is a parabola (rightward parabola), but the temperature difference for the irregular test section duct differed linearly in the flow direction. The temperature difference distribution of $y_1=6.5$ cm is more uniform than $y_2=13$ cm and $y_3=19.5$ cm; however, the temperature difference distribution of an irregular test segment duct is stronger at $y_1=6.5$ cm. The Nusselt number is inversely influenced by the relative longitudinal pitch. With increasing relative longitudinal pitch, the Nusselt number decreases by adding all kinds of wavy winglets on the absorber plate, i.e. it is more for 3 and less for 6 relative longitudinal pitch. It is found that the Nusselt number is the limit for 5 wave numbers. This trend is seen in all the relative longitudinal values.

REFERENCES

- [1] L.Z. Zhang, and Z.Y. Chen, "Convective heat transfer in cross-corrugated triangular ducts under uniform heat flux boundary conditions", *International Journal of Heat and Mass Transfer*, Vol. 54, No. 1-3, Pp. 597-605, 2011.
- [2] K. Sivakumar, E. Natarajan, and N. Kulasekharan, "Heat transfer and pressure drop comparison between smooth and different sized rib-roughened rectangular divergent ducts", *International Journal of Engineering and Technology (IJET)*, Vol. 6, No. 1, Pp. 263-272, 2014.
- [3] L.Z. Zhang, and Z.Y. Chen, "Convective heat transfer in cross-corrugated triangular ducts under uniform heat flux boundary conditions", *International Journal of Heat and Mass Transfer*, Vol. 54, No. 1-3, Pp. 597-605, 2011.
- [4] N. Onur, and K. Arslan, "Experimental investigation of laminar heat transfer inside trapezoidal duct having different corner angles", *Experimental Heat Transfer*, Vol. 28, No. 1, Pp. 89-105, 2015.
- [5] M. Renksizbulut, and H. Niazmand, "Laminar flow and heat transfer in the entrance region of trapezoidal channels with constant wall temperature", 2006.
- [6] R. Bhadouriya, A. Agrawal, and S.V. Prabhu, "Experimental and numerical study of fluid flow and heat transfer in a twisted square duct", *International Journal of Heat and Mass Transfer*, Vol. 82, Pp. 143-158, 2015.
- [7] F. Liu, "Effects of geometries on heat transfer enhancement of thermal fluids in curved ducts", *Applied Thermal Engineering*, Vol. 90, Pp. 590-595, 2015.

- [8] X. Zhang, Y. Wang, R. Jia, and R. Wan, "Investigation on heat transfer and flow characteristics of heat exchangers with different trapezoidal ducts", *International Journal of Heat and Mass Transfer*, Vol. 110, Pp. 863-872, 2017.
- [9] N. Tokgoz, "Experimental and numerical investigation of flow structure in a cylindrical corrugated channel", *International Journal of Mechanical Sciences*, No. 157, Pp. 787-801, 2019.
- [10] M. Norouzi, M.H. Kayhani, C. Shu, and M.R.H. Nobari, "Flow of second-order fluid in a curved duct with square cross-section", *Journal of Non-Newtonian Fluid Mechanics*, Vol. 165, No. 7-8, Pp. 323-339, 2010.
- [11] M.M. Shahmardan, M. Norouzi, M.H. Kayhani, and A.A. Delouei, "An exact analytical solution for convective heat transfer in rectangular ducts", *Journal of Zhejiang University SCIENCE A*, Vol. 13, No. 10, Pp. 768-781, 2012.
- [12] R.H.K. KC, "A Mechanism for Selection of Screw-Type Dental Implants for Patients with Low-Density and Osteoporotic Bone (Doctoral dissertation, University of Central Oklahoma)", 2020.
- [13] H.C. Chiu, J.H. Jang, and W.M. Yan, "Mixed convection heat transfer in horizontal rectangular ducts with radiation effects", *International Journal of Heat and Mass Transfer*, Vol. 50, No. 15-16, Pp. 2874-2882, 2007.
- [14] B. Farhanieh, and B. Sunden, "Three-dimensional laminar flow and heat transfer in the entrance region of trapezoidal ducts", *International journal for numerical methods in fluids*, Vol. 13, No. 5, Pp. 537-556, 1991.
- [15] M. Ghobadi, and Y.S. Muzychka, "A review of heat transfer and pressure drop correlations for laminar flow in curved circular ducts", *Heat Transfer Engineering*, Vol. 37, No. 10, Pp. 815-839, 2016.
- [16] Y.L. He, P. Chu, W.Q. Tao, Y.W. Zhang, and T. Xie, "Analysis of heat transfer and pressure drop for fin-and-tube heat exchangers with rectangular winglet-type vortex generators", *Applied Thermal Engineering*, Vol. 61, No. 2, Pp. 770-783, 2013.
- [17] D. Grosso, A.A. de, G.J. Soler-Illia, F. Babonneau, C. Sanchez, P.A. Albouy, A. Brunet-Bruneau, and A.R. Balkenende, "Highly organized mesoporous titania thin films showing mono-oriented 2D hexagonal channels", *Advanced Materials*, Vol. 13, No. 14, Pp. 1085-1090, 2001.
- [18] A.A.A. Arani, A. Arefmanesh, and A. Niroumand, "Investigation of fully developed flow and heat transfer through n-sided polygonal ducts with round corners using the Galerkin weighted residual method", *Int. J. Nonlinear Anal. Appl.*, Vol. 9, No. 1, Pp. 175-193, 2018.